Polymer 50 (2009) 5749–5757

Contents lists available at ScienceDirect

Polymer

journal homepage: www.elsevier.com/locate/polymer

The synthesis, characterization and biocompatibility of poly(ester urethane)/polyhedral oligomeric silesquioxane nanocomposites

Wenshou Wang [a], Yan-lin Guo [b], Joshua U. Otaigbe [a,*]

[a] School of Polymers & High Performance Materials, The University of Southern Mississippi, Hattiesburg, MS 39406-0076, United States
[b] Department of Biological Sciences, The University of Southern Mississippi, Hattiesburg, MS 39406-0076, United States

ARTICLE INFO

Article history:
Received 20 January 2009
Received in revised form
5 May 2009
Accepted 19 May 2009
Available online 27 May 2009

Keywords:
Poly(ester urethane)s
Polyhedral oligomeric silesquioxanes
Biocompatibility and cytotoxicity

ABSTRACT

The primary goal of this study is to develop a facile and inexpensive synthesis method for a new biodegradable and biocompatible poly(ester urethane) (PEU)/polyhedral oligomeric silesquioxanes (POSS) nanocomposite via *in situ* homogeneous solution polymerization reaction into prescribed macromolecular structure and properties including improved biocompatibility, thermal and hydrolytic stability, and stiffness and strength. Cell culture studies, nuclear magnetic resonance spectroscopy, X-ray diffraction, differential scanning calorimetry, thermogravimetry, and dynamic mechanical analysis measurements were used to confirm the structure and property improvements. The results show that the targeted PEU/POSS nanocomposites (which are remarkably different from conventional polymers, polymer nanocomposites and microcomposites) have significant improvements in mechanical properties and degradation resistance at small POSS concentrations ($\leq$6 wt%). The nanocomposites exhibited excellent support for cell growth without any toxicity. POSS concentration did not affect cell adhesion or cell growth, but it significantly changed the surface structure of the PEU into a 3-dimensional matrix with regular pores that may allow cells to better access the growth factors/nutrients, waste exchange, and tissue remodeling. The PEU/POSS nanocomposites were resistant to degradation over a period of six months when exposed to a buffer solution. These desirable characteristics suggest that the nanocomposites may hold great promise for future high-end uses such as in biomedical devices, especially at cardiovascular interfaces.

Published by Elsevier Ltd.

1. Introduction

One motivation for the present study is from the work on nanostructured polymer blends previously reported by Otaigbe and co-workers [1–3]. In that work, the feasibility of making nanostructured polymer blends directly from *in situ* simultaneous polymerization and compatibilization of reactive cyclic monomers in the presence of a compatible molten polymer was demonstrated [1–3]. In this nanostructured polymer blend the scale of dispersion of the one polymer phase in the other was $<$100 nm. Another motivating factor for the work described in the present article is the reported quantal properties of silica nanocomposites containing reactive polyhedral oligomeric silsesquioxanes (POSS) as a result of their unique physical characteristics [4–6] previously not possible because of classical physical laws [7]. POSS, as a nanoscale hollow cage structure of Si, with the bioactivity and other physical properties of porous Si [8,9], should have similar biocompatibility and bioactivity. Therefore, there is currently a significant research interest in introducing POSS into biodegradable polyurethanes [10,11] to yield biocompatible and relatively inexpensive biomaterials for possible uses in tissue engineering [12–16]. It is worthy to note that rational synthesis and processing of these materials plays a crucial role in determining the final polurethane/POSS nanocomposite product performance in a number of biomedical applications areas.

Recently, Seifalian and co-workers [6] reported new evidence that these silica nanocomposites may also extend into the world of biology and medicine such as in cardiovascular interventional devices, making the materials science concept potentially widely applicable. For example, it is well known that blood vessel development is a complex process that requires endothelial cell proliferation, differentiation, and assembly into the tube-like structures. This process critically depends on the interaction between endothelial cells and extracellular matrix (ECM) that supports the cell growth. Although much work in the field uses natural biopolymers for basic research, the unavailability and complexity of the natural ECM materials significantly limit their potential for biomedical application. Consequently, there is an increasing need to develop

* Corresponding author. Tel.: +1 601 266 5596.
E-mail address: joshua.otaigbe@usm.edu (J.U. Otaigbe).

0032-3861/$ – see front matter Published by Elsevier Ltd.
doi:10.1016/j.polymer.2009.05.037

biocompatible synthetic polymers as substitutes for the natural ECM materials. A prerequisite for any biomedical application of synthetic polymers is their biocompatibility with the targeted tissues and organs, in addition to their basic chemical and mechanical properties. In a previous paper [17], we showed that pure PEU does not have apparent toxicity on three cell types tested, endothelial cells, epithelial cells and stem cells, indicating its broad compatibility with different cells. In the current paper, we investigated the effects of POSS content on the structure and biocompatibility of PEU/POSS nanocomposite as a critical prerequisite for the potential application of the PEU/POSS nanocomposite in manufacturing biomedical devices, such as materials for stents and artificial vessels in cardiovascular tissue engineering.

In the past, incorporation of silicon into polymers has been in the form of siloxane, which in itself is noncompliant as a result of elasticity mismatch of the composite constituents [18,19]. The philosophy of the present study is to explore the feasibility of an alternative approach of incorporating very small amounts of silicon in the form of special nanoscale reactive POSS molecules as an integral part of polyurethane chain segments which would preserve the favorable properties (e.g. improved stiffness, strength, thermal stability and biocompatibility) of the hybrid polyurethane/POSS nanodispersions and compliance of the resulting solid-state hybrid polyurethane/POSS nanocomposite while significantly lowering its surface tension properties [20,21]. The resulting polyurethane/POSS nanocomposite materials are expected to possess improved properties such as lower surface tension [20] and lower bacterial adhesion than that of current synthetic biomaterials (e.g., PTFE) used in biomedical devices [22]. POSS is made directly from silicones, silanes and a limited number can even be prepared from silica. As structurally well-defined silicon-based molecules, they can be reactively compounded and/or nonreactively blended into a wide variety of functionalities suitable for polymerization, grafting, surface bonding, and other transformations [23–26]. POSS silicon–oxygen framework ($SiO_{1.5}$) is intermediate between that of a silicone (SiO) and silica (SiO_2). This imparts excellent oxidative stability and thermal resistance. The carbon "R" groups (*organic*) located on the silicon atoms aid in the solubilization and compatibilization of the POSS cage with organic resins, biological systems, and surfaces. The overall three-dimensional nature of POSS nanostructures is nearly equivalent in size, 0.7–3 nm (ave. = 1.5 nm) to most polymer dimensions. Thus, when incorporated into a polymer at a molecular level, POSS can effectively control chain motion, glass transition and other physical properties. Structural control at this length-scale has not previously been possible, yet it is at the nanoscopic length scale that a wide number of physical properties originate [27]. Therefore the high surface area of POSS allows it to readily interact with a large number of polymer chains at relatively low loadings (from 1 to 10 wt%) [20,27–30].

The current work described in this article is part of a long-range research program that envisions that the behavior of these interesting biodegradable and biocompatible PEU/POSS nanocomposite materials is governed by the method of nano-reinforcement, the nano-interface, the synthetic process utilized, its microstructural effects, and the interaction between the PEU and POSS components. The present study focuses on preparing and characterizing biodegradable and biocompatible poly(ester-urethane)/POSS (PEU/POSS) nanocomposites through homogeneous solution polymerization. The PEU/POSS nanocomposite films will be obtained from melt processing of the as-synthesized PEU/POSS nanocomposites *without* using processing aids or modifiers (lubricants) that can negatively impact surface properties such as biological activity and antibacterial surface action of the resulting nanocomposite materials. A special reactive diol-POSS was used to obtain new PEU/POSS nanocomposites by using a highly efficient catalyst, resulting in improved biocompatibility, biodegradation rate, and thermomechanical properties. This study may stimulate a better understanding of the proposed rational synthesis of biodegradable and biocompatible polyurethane materials with improved properties and biological function not now possible, making them widely applicable. Our data also provide a quantitative experimental basis for future detailed structure/property studies of the relatively new hybrid PEU/POSS nanocomposite films aimed at the prediction of their properties and biological function, increasing our level of understanding of the behavior of these systems and other similar polymers. Therefore, it is likely that increased attention by other researchers will be focused on these materials in the future.

2. Materials and methods

2.1. Materials

Poly(ε-caprolactone) diol (TONE® Polyol 5249) was purchased from Dow Chemical Company and the methylenediphenyl diisocyanate (MDI), toluene, dibutyltin dilaurate and 1,4-butanediol were obtained from Sigma–Aldrich. 1,2-Propanediolisobutyl POSS (AL0130) was donated by Hybrid Plastics, Hattiesburg, MS. Phosphate Buffer Solution (1 M, pH = 7.4) was purchased from Sigma–Aldrich Company. The polyol and MDI were dried in a vacuum oven at 40 °C for 24 h prior to use.

2.2. Synthesis of poly(ester urethane)/POSS nanocomposites

A 100 ml round-bottomed three-necked flask equipped with a magnetic stirrer was used as a reaction vessel for the polymerization reaction whose temperature was controlled by using a constant temperature oil bath. Desired amounts of poly(ε-caprolactone) diol, POSS diol, toluene, and methylenediphenyl diisocyanate were added to the flask (see Table 1). The flask was then immersed in the oil bath maintained at 60 °C and its contents stirred under a nitrogen atmosphere. After the solid contents dissolved completely, dibutyltin dilaurate (1 wt% of the total weight) was added to the reaction system. A relatively high concentration of dibutyltin dilaurate was necessary due to the low reactivity of the POSS diol used. After 3 h, 1,4-butanediol was added to the flask as chain extender. The overall molar ratio of hydroxyl to isocyanate functional groups is 1:1.05. The reaction was allowed to continue for another 5 h while maintaining the temperature at 60 °C. The reaction product was precipitated into ethanol and dried in a vacuum oven at 40 °C for 48 h. Subsequently, the dried products were compression molded at 143 °C into test specimens with desired shapes for the following measurements except the cell culture culture and cytotoxicity analysis. Note that thin films that were prepared via solution casting were used for the cell culture and cytotoxicity analysis.

2.3. NMR spectroscopy

Liquid phase ^{1}H NMR measurements were performed at room temperature on the PEU/POSS nanocomposite using a Mercury 300

Table 1
The feed ratio of the samples and their molecular weights.

Sample	PCL diol (g)	POSS diol (g)	MDI (g)	BDO (g)	$M_w \times 10^4$ g/mol	$M_n \times 10^4$ g/mol
PEU	10	0	4.33	1	3.51	1.67
PEU/1.5%POSS	9.75	0.25	4.37	1	4.02	1.74
PEU/3%POSS	9.5	0.5	4.41	1	3.38	1.77
PEU/4.5%POSS	9.25	0.75	4.45	1	3.68	1.80
PEU/6%POSS	9	1	4.49	1	4.27	1.84

spectrometer operating at 300 MHz with (methyl sulfoxide)-d_6 as solvent, following standard procedures.

2.4. X-ray diffraction

The crystallinity of the PEU/POSS nanocomposite was evaluated using X-ray diffraction (XRD) analysis. A Rigaku Ultima® III powder diffractometer was used, employing Cu Kα radiation (at 40 kV and 44 mA). Data were collected over the range of $2\theta = 3$–35° at a rate of 1°/min.

2.5. DSC and TGA measurements

Differential scanning calorimetry (DSC) was carried out on the samples over a temperature range of -80 °C to 250 °C using a TA Instruments (TA Q100) operating under a nitrogen atmosphere. The DSC heating or cooling rate was 10 °C/min. The midpoint of the transition zone was taken as the glass transition temperature (T_g) of the sample. Thermogravimetric analysis (TGA) tests were conducted on the samples using a Perkin–Elmer (Pyris 1 TGA) equipment operating from 50 °C to 800 °C at a heating rate of 10 °C/min and under a nitrogen atmosphere. Thermal decomposition temperature was defined as the temperature corresponding to the maximum rate of weight loss.

2.6. Static and dynamic mechanical measurements

Static mechanical tensile stress–strain measurements were performed on the samples using a Material Testing System Alliance RT/10 and a MTS Testworks 4 computer software package for automatic control of test sequences and data acquisition and analysis. Dumbbell-shaped test specimens (with an effective cross-section of 4×0.7 mm^2) were cut from the compression molded PEU/POSS sheets and tested at room temperature using a crosshead speed of 20 mm/min according to the ASTM D882-88 standard method. The tests were performed in triplicate to give mean values reported in this paper.

The temperature dependencies of the storage moduli E' and mechanical damping ($\tan\delta$) of the compression molded rectangular test specimens ($20 \times 5 \times 1$ mm^3) were determined using a PYRIS Diamond® Dynamic Mechanical Analyzer (DMA) operating at temperatures ranging from -80 °C to 150 °C at a heating rate of 3 °C/min, a frequency of 1 Hz, and a linear strain amplitude of 10%.

2.7. Degradation in buffer solution

Degradation tests on the molded samples were conducted in a buffer solution of pH = 7.4 at a degradation temperature of 37 °C following our previously reported procedures [17].

2.8. Cell culture and cytotoxicity analysis

Three types of cells were used in this study; human umbilical vein endothelial cells (HUVECs), mouse embryonic stem cells (mESCs) and human KB cells (an epithelial cell line derived from a human carcinoma of the nasopharynx). The cell culture conditions have been described previously [17]. Similar results were obtained from the three types of cells tested. The data presented in this study were obtained from experiments using KB cells. Microscopic coverglasses were coated with PEU or PEU/POSS thin films, which served as cell growth matrices. For cell proliferation assay, KB cells were grown on the coverglasses in 24-well cell culture dishes at a density of 5×10^3/ml. The cells were cultured in RPMI medium that contained 10% fetal bovine serum. After incubation for 48 h at 37 °C in a humidified incubator (5% CO_2, 95% air), the cells were fixed and stained with 1% toluidine blue as previously described [17]. Cells were washed extensively with water and examined under an Olympus microscope with a phase contrast lens and photographed with a Cannon digital camera. To quantitatively determine cell number, toluidine blue was extracted with 2%

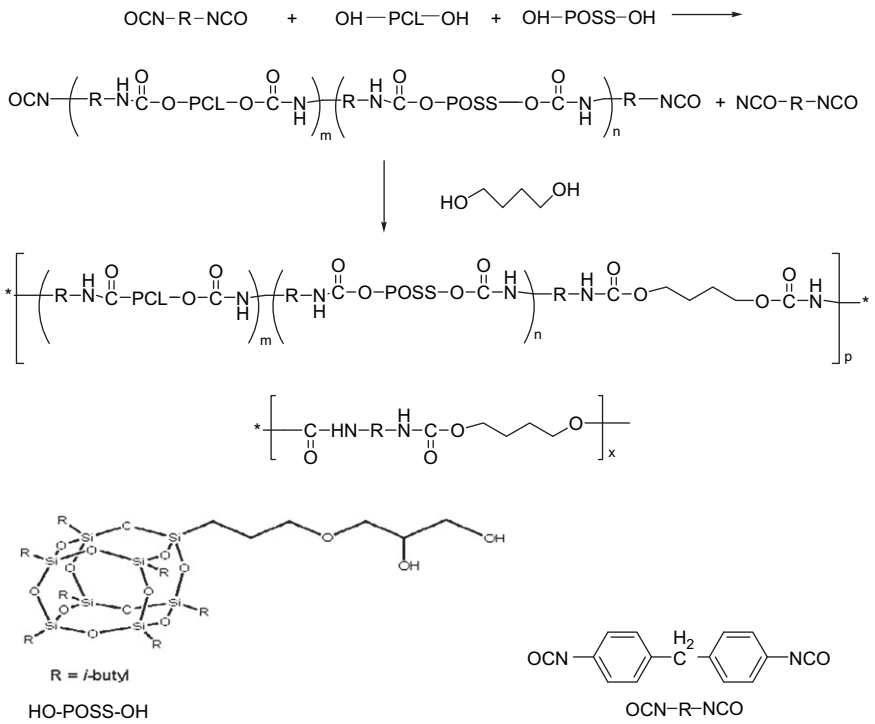

Scheme 1. The synthesis route of poly(ester urethane)/POSS nanocomposites.

sodium dodecyl sulfate. The absorbance at 630 nm, which correlates with cell number, was measured with a microtiter plate reader. For cell adhesion analysis, 1×10^4 KB cells were seeded on different matrices in 24-well cell culture dishes. The cells were incubated for 2 h and then fixed. The number of attached cells was determined by the same method as described for cell proliferation assay.

2.9. Microscopic analysis of PEU/POSS matrix structure and cell–matrix interaction

To further analyze the cell morphology and their interaction with PEU or PEU/POSS matrices, cells were double stained with 1% toluidine blue and 10 μM 4′,6-diamidino-2-phenylindole (DAPI, a DNA binding dye). The nuclei stained with DAPI emit bright blue color under a fluorescent microscope. The cells were examined under an Olympus fluorescence microscope (BX60, UplanFl 100×/1.30 oil lens) with filters set for the examination of DAPI staining. The images were photographed with a micropublisher digital camera (Qimaging). To visualize the auto-fluorescence of the polymer films, the samples were examined under a Nikon fluorescence microscope (Eclipse 80i, Plan Fluor 10X/0.75 DIC M/N2 lens) with filters set for the examination of fluorescein isothiocyanate (FITC). The images were processed using Image-Pro Plus software.

3. Results and discussion

3.1. The synthesis of PEU/POSS nanocomposites

Five samples of PEU/POSS nanocomposites with different POSS content were synthesized as already described above. Elementary steps of the synthetic reaction route are shown in reaction Scheme 1. The molecular weights of the samples were measured by gel permeation chromatography (GPC) using THF as solvent and polystyrene as standard. The weight-average (M_w) and number-average (M_n) molecular weights obtained are listed in Table 1. The table shows that the molecular weights of samples were little affected by the presence of the POSS, showing an approximate polydispersity ratio (M_w/M_n) of about 2.14.

3.2. Structure of PEU/POSS nanocomposites

NMR and XRD were used to characterize the molecular structures of the PEU and the PEU/POSS nanocomposites. Fig. 1 shows the NMR spectra of POSS, PEU and PEU/POSS nanocomposites. The observed NMR peaks are assigned as follows: 0 ppm (tetramethylsilane), 3.3 ppm (H_2O), 2.5 ppm (dimethyl sulfoxide), 0.9 ppm (methyl in the POSS), 0.61 ppm (–Si–CH_2–CH–), 7.1 ppm and 7.3 ppm (benzene ring of MDI), 9.5 ppm (hydrogen in urethane group), 3.8 ppm (methylene in MDI and BDO), 1.5 ppm (methylene in BDO and poly(ε-caprolactone) (PCL)). The remaining peaks are assigned to the incorporated PCL segment in the PEU/POSS nanocomposite. The NMR data are consistent with our expectation of direct incorporation of the POSS moieties in the backbone macromolecular chain structure of the PEU.

Fig. 2 shows the XRD data of the PEU and PEU/POSS nanocomposites at the POSS concentrations indicated. Two relatively sharp crystalline peaks at $2\theta = 6.7^\circ$ and $2\theta = 21.0^\circ$, corresponding to the PCL crystal, were observed for the pure PEU. Clearly the figure shows that incorporation of POSS in the PEU strongly affects the crystal peaks just mentioned. No sharp crystalline peaks around $2\theta = 21^\circ$ were observed for the PEU/POSS nanocomposites with POSS content of 1.5 wt% and 3 wt% (only broad peaks are evident) while the peaks at $2\theta = 6.7^\circ$ were observed to shift to $2\theta = 7.0^\circ$ and

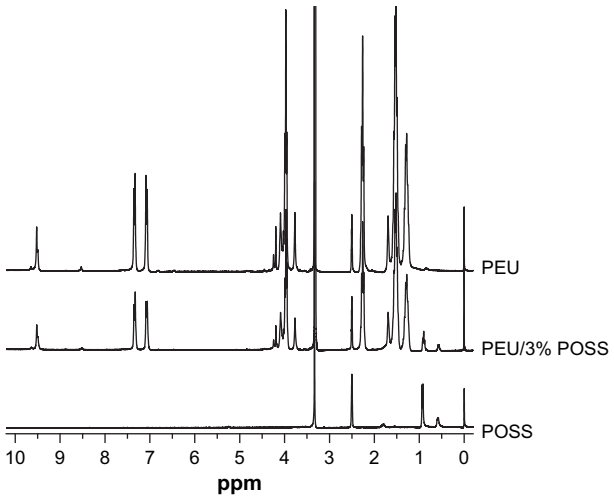

Fig. 1. NMR spectra of PEU, POSS and PEU/POSS nanocomposites.

$2\theta = 7.1^\circ$, respectively. When the POSS content was increased to 6 wt%, three peaks at $2\theta = 7.1^\circ$, 19.7° and 21.3° were observed. These results indicate that low POSS concentrations (≤3 wt%) decrease the crystallinity of the PEU soft segment and consequently improve the compatibility between the soft and hard segments of the PEU. In addition, the results are consistent with the formation of POSS nanocrystals in the PEU hard segment (especially at high POSS

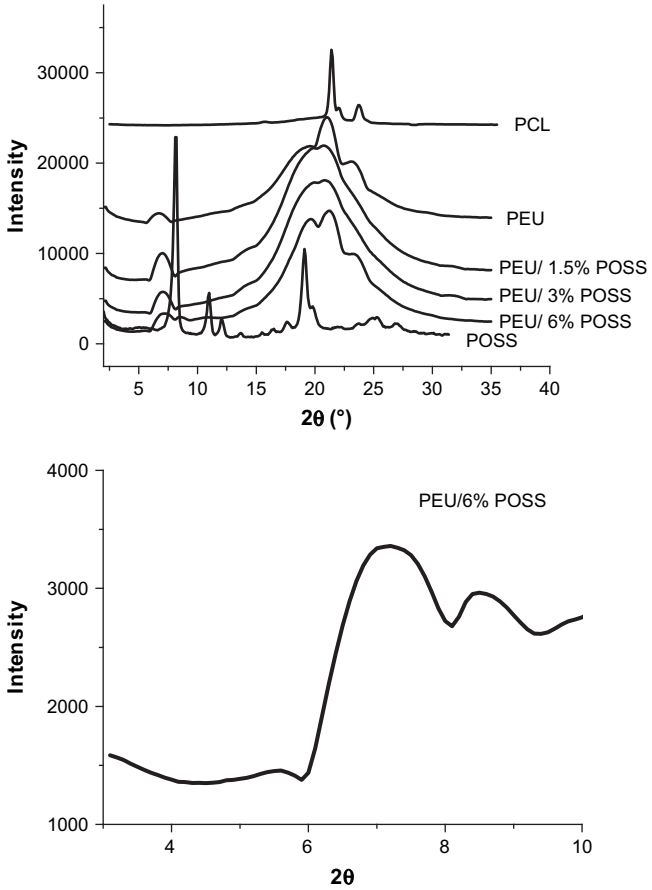

Fig. 2. XRD spectra of PEU and PEU/POSS nanocomposites. The bottom figure is a magnified portion of the PEU/6% POSS in the 2θ range of 2–10° shown in the top figure.

concentration) as previously reported by Fu et al. [31]. This improved compatibility facilitates the physicochemical interaction between soft and hard segments as confirmed by the increase of glass transition temperature discussed in the next section.

3.3. Thermal analysis

DSC was used to measure the thermal properties of the PEU/POSS nanocomposites. The glass transition temperatures of the nanocomposites were found to increase with increasing POSS content from a $T_g = -22\,^{\circ}C$ (pure PEU) to a $T_g = -15\,^{\circ}C$ (PEU/POSS with 6 wt% POSS) as shown in Fig. 3. This finding is thought to be due to the relatively rigid POSS (which is chemically inserted into the PEU macromolecular chain structure) restricting the molecular chain motion thereby decreasing the free volume. Another plausible explanation of the POSS effect on T_g is ascribed to the POSS restricting the motion of the crystalline PCL moieties in the POSS-modified PEU structure and may consequently frustrate its phase separation thereby significantly enhancing the interaction between hard and soft segments of the PEU. The free volume decrease and frustration of phase separation effects are well known factors that lead to increasing glass transition temperatures of synthetic polymers and blends [32,33].

The thermal stability of the molded PEU/POSS nanocomposites was tested by TGA. Fig. 4 shows that the thermal decomposition temperature is 314 °C for the pure PEU, increasing with POSS content (up to 328 °C for the 6 wt% POSS content). This observation is consistent with the reported tendency of POSS to increase the thermal stability of polymers [34,35]. In the present work the thermal stability enhancement exhibited by the nanocomposites is believed to be due to the restriction of the thermal motions of the tethered PEU/POSS macromolecular chain structure, reducing the organic decomposition pathways accessible to the tether. In addition, the inorganic POSS component provides additional heat capacity thereby stabilizing the materials against thermal decomposition [36,37].

3.4. Mechanical properties

Fig. 5 shows typical stress–strain curves and the dependencies of the tensile strength, modulus and elongation at break on POSS content for the PEU/POSS nanocomposites studied. The figure shows an approximately linear increase of tensile strength with increasing POSS content of the nanocomposites. The maximum 6 wt% POSS content studied showed about 71% increase in the tensile strength of the pure PEU. A relatively moderate increase in the modulus and a relatively insignificant effect on elongation at break of the nanocomposites with increasing POSS content is clearly evident in Fig. 5. DMA was used to study the temperature dependencies of the moduli of the PEU and PEU/POSS nanocomposites and the results obtained are shown in Fig. 6. Clearly, this figure shows that the PEU/POSS nanocomposites have higher modulus than that of the pure PEU over the temperature range investigated. The improvement of mechanical properties of the PEU/POSS nanocomposites is ascribed to the nanoscale reinforcement of the molecular POSS cage in the PEU matrix [38]. Fig. 6b illustrates the temperature dependencies of tan δ for the pure PEU and PEU/POSS nanocomposites. The temperature corresponding to the maxima of the tan δ peaks (i.e., T_g of the PEU soft segment) appears to be relatively unaffected by the presence of POSS. But the intensities of the tan δ peaks were significantly increased by the incorporation of 3 and 6 wt% POSS, suggesting contributions of additional molecular relaxation processes. The discrepancy between the T_gs obtained from the DMA and DSC data is due to the fact that the mechanisms responsible for the glass transition process observed in DSC are different from the molecular relaxation processes probed by DMA. Despite this discrepancy, the data at hand confirm that the POSS is preferentially chemically reacted with the PEU hard segment as previously reported [21]. Extensive correlation of the structure dynamics and their molecular origins with the biological function of the POSS-modified PEU is needed to allow tuning the materials to specific macromolecular structure and function. This is a matter for future investigation.

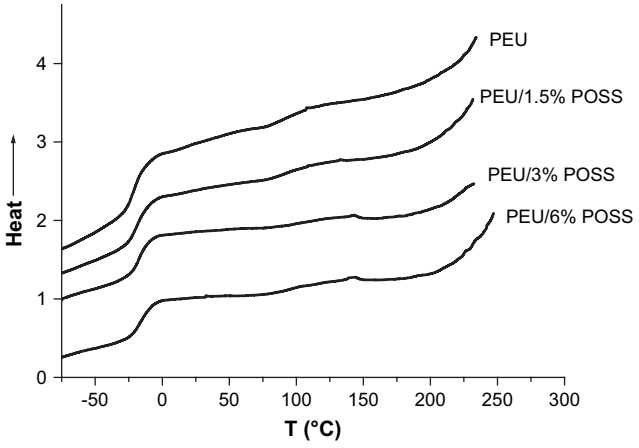

Fig. 3. DSC heating curves of PEU and PEU/POSS nanocomposites.

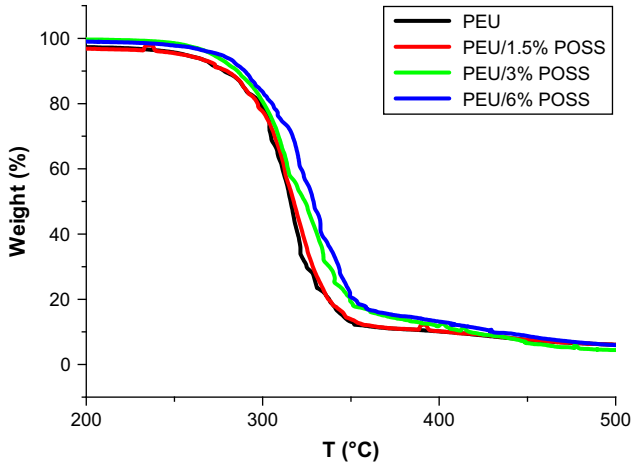

Fig. 4. TGA weight loss as a function of temperature of PEU and PEU/POSS nanocomposites.

3.5. Degradation of PEU/POSS in buffer solution

The effect of POSS on the degradation behavior of the PEU/POSS nanocomposites was studied via degradation tests in buffer solution according to previously reported procedures [17]. No measurable weight loss was observed for both PEU and PEU/POSS nanocomposites after an elapsed time of six months, indicating very slow degradation in the buffer solution and absence of very small molecular weight species (e.g., unreacted monomers, oligomers) leaching out of the sample in the experimental time period investigated. After six months the samples showed some evidence of cracking, therefore, we decided to measure their molecular weights by gel permeation chromatography after exposure to the buffer solution for specified time periods and the results obtained are shown in Fig. 7. This figure shows variation of weight-average

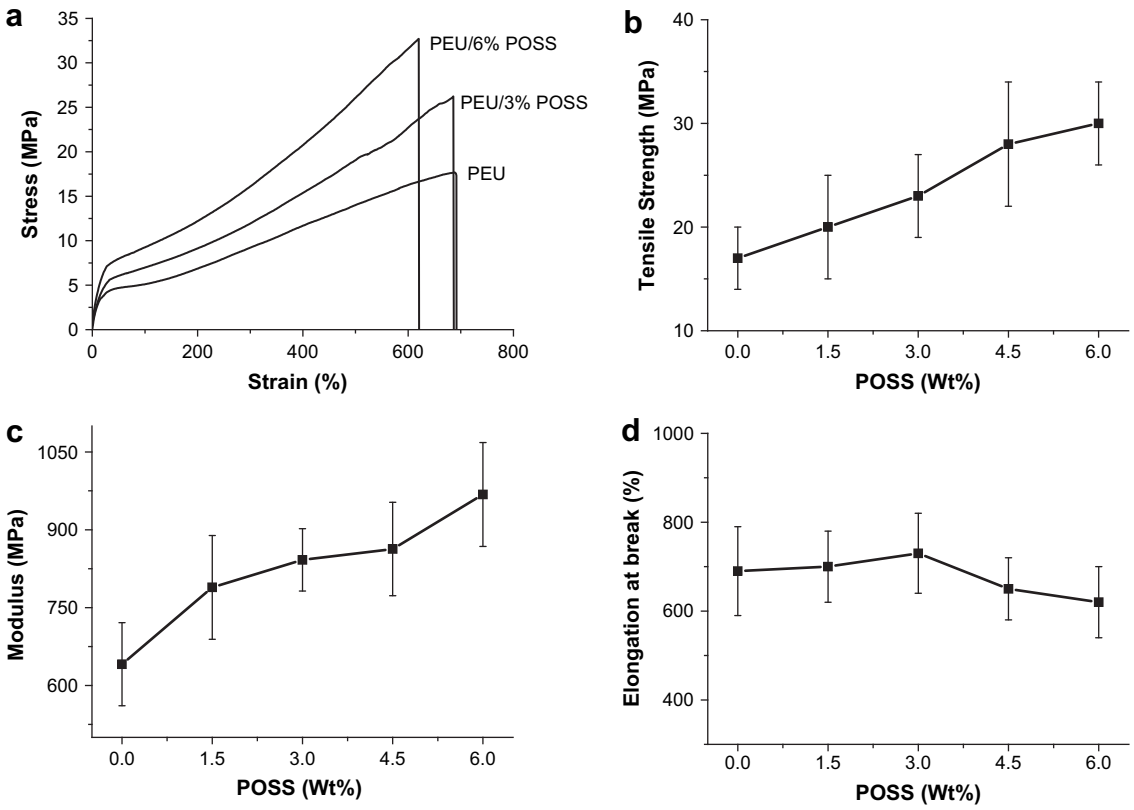

Fig. 5. Tensile stress–strain data of PEU and PEU/POSS nanocomposites: (a) typical stress–strain curves, (b) tensile strength, (c) modulus, and (d) elongation at break versus POSS concentration.

molecular weight with elapsed time for the nanocomposites after exposure to the buffer solution. For the pure PEU, the weight-average molecular weight decreased from 3.5×10^4 to 1.5×10^4 g/mol (i.e., about 57% decrease). Incorporation of the 3 and 6 wt% POSS into the PEU resulted in molecular weight decrease of 50% (3 wt% POSS) and 44% (6 wt% POSS), respectively, indicating that incorporation of POSS into the PEU may be used to increase the water resistance of the latter like Seifalian and co-workers have reported for other types of polyurethanes [39]. The ability of POSS to increase water resistance in PEU/POSS nanocomposite is thought to be due to the silsesquioxane nanocores shielding the soft segments of the polyurethane responsible for its compliance and elasticity [39].

3.6. Cell growth, surface topography of PEU/POSS matrices, and cell-matrix interaction

The preceding results show that incorporation of POSS into PEU alters a number of chemical and physical properties of the latter. Therefore, it is interesting to test how these changes will affect biocompatibility and cell behavior. We seeded cells on the thin film matrices formed from PEU, PEU/3 wt% POSS, and PEU/6 wt% POSS. No apparent toxicity was detected within a 48 h incubation period in comparison with the cells grown on conventional cell culture dishes, which was used as a control for comparison. After fixation and stained with toluidine blue, the cells were easily identified by their dark purple color (Fig. 8A, photo). Incorporation of POSS into PEU did not significantly affect cell proliferation and cell viability since the cell densities were similar in all three films tested. This was confirmed by the quantitative measurement of toluidine blue extracted from the stained cells, which correlates with the cell number (Fig. 8A, graph). The cells could grow to a near confluent monolayer in a longer incubation period (data not shown). To analyze the effect of incorporation of POSS into PEU on the initial cell attachment, we seeded the cells onto PEU and PEU/POSS (6 wt%) thin films, standard cell culture plate (tissue-culture treated polystyrene surface) or uncoated coverglass (Glass) for comparison. The numbers of attached cells were determined after 2 h incubation. As shown in Fig. 8B, both PEU and PEU/POSS film showed higher cell adhesion capacity than the surface of cell culture plate (TCP) with PEU/POSS having slight improvement for cell adhesion than PEU, while uncoated coverglass (Glass) showed the least ability to promote cell adhesion. Numerous studies have demonstrated that PU support cell adhesion and proliferation [12]. It has been shown for PU that a number of factors, such as the ratio of hard to total segment concentration and the recrystallization temperature influence cell adhesion and proliferation [40]. But it is not clear exactly what chemical groups of the polymers are responsible for interaction with cells. In the current study, the reasons for the observed difference in cell adhesion between PEU and PEU/POSS are presently unknown. Nevertheless, it is clearly evident from the experimental results already discussed that the incorporation of POSS into PEU does not compromise the ability of PEU in promoting cell adhesion and cell proliferation.

To further analyze the detail structure of the cells and their interaction with the polymer matrices, we examined the samples under a microscope at high magnification. We double stained the cells with toluidine blue (TB), which stained whole cell dark purple under a phase contrast lens, and DAPI, which stains the nuclei with bright blue color under a fluorescent lens. As shown in Fig. 9, when cells were grown on the surface of conventional glass cell culture plates, the cells exhibited flattened morphology (Fig. 9, A, TB) with crisply defined round nuclei (Fig. 9, a, DAPI). On the other hand, the polymer thin films formed porous matrices in which cells were

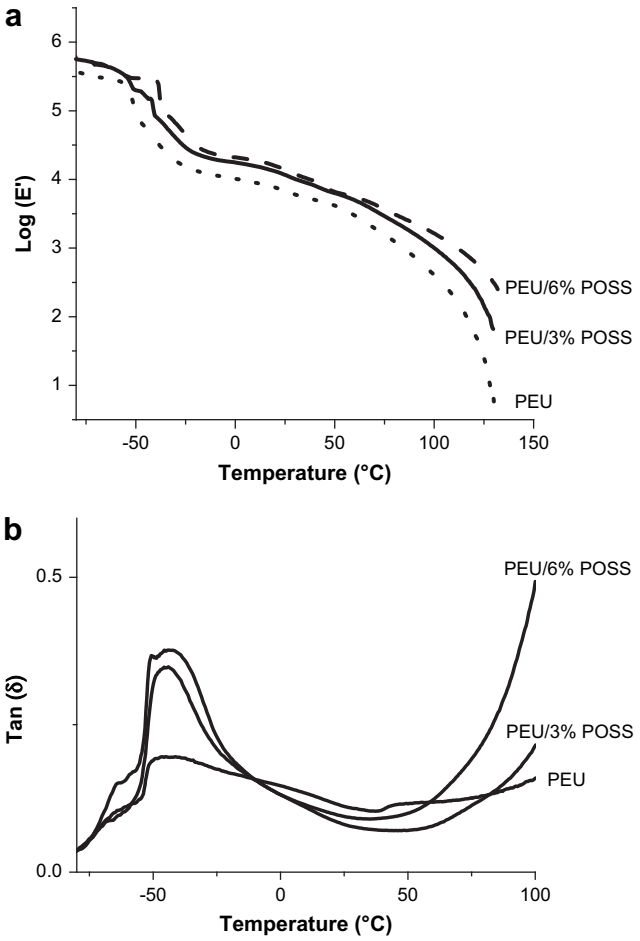

Fig. 6. Temperature dependencies of moduli (a) and mechanical damping (tan δ) (b) of PEU and PEU/POSS nanocomposites.

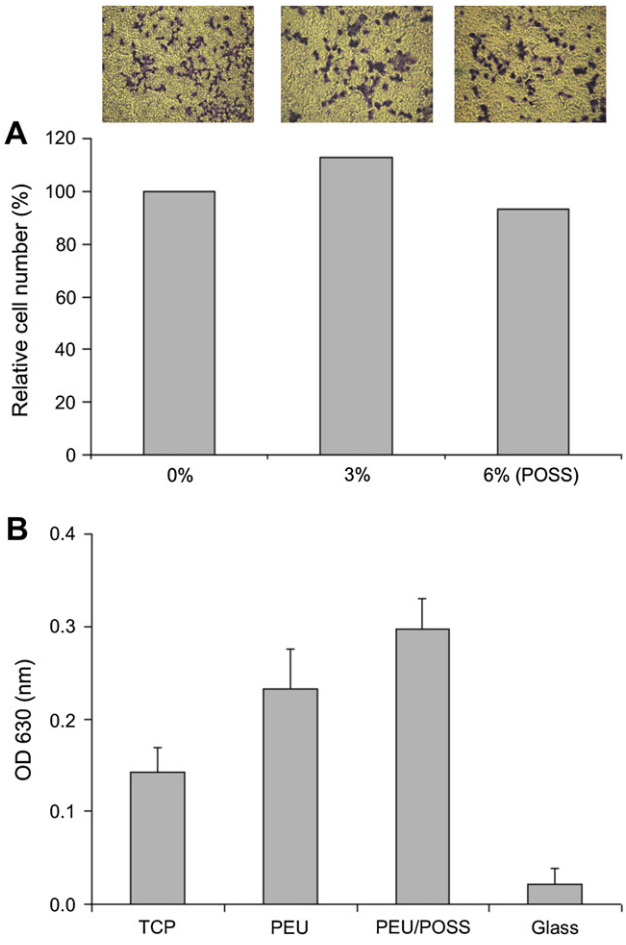

Fig. 8. Cell proliferation and adhesion on PEU and PEU/POSS thin film matrices. KB cells were grown on the polymer thin firms as indicated. For cell proliferation assay (A), cells were fixed and stained with 1% toluidine blue (TB) and examined under a phase contrast microscope (photos) after 48 h culture. To quantitatively measure cell numbers, TB was extracted from the stained cells. The absorbance, which correlates with the cell number, was measured at OD 630 nm. The value obtained from cells grown on PU film (0% POSS) was set as 100%. The values are means of duplicate assays. For cell adhesion assay (B), cells were fixed and stained with 1% TB after 2 h incubation. The numbers of attached cells are indirectly measured by the absorbance at 630 nm. The values are means ± SD of triplicate assays.

partly embedded as revealed after TB cell staining (Fig. 9, B, C, D, TB). The nuclei were detected with different intensities of bright blue fluorescence and blur images, indicating that they were located at different planes (Fig. 9, b, c, d, DAPI, indicated by arrows). Interestingly, the fluorescent microscope also revealed the fine structure of the polymers by their auto-fluorescence; pure PEU mainly detected as loosely connected large particles (Fig. 9,b) while

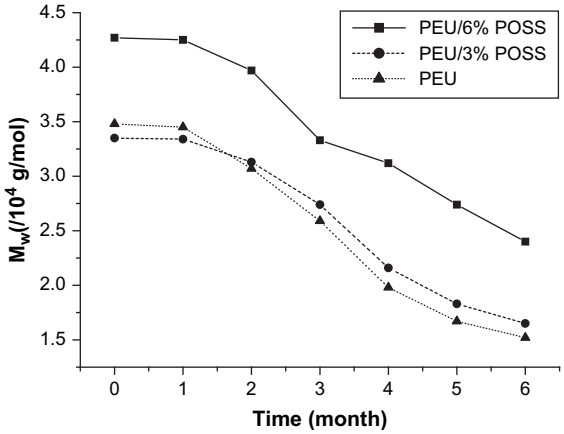

Fig. 7. Weight-average molecular weight versus exposure time in buffer solution for the PEU and PEU/POSS nanocomposites as described in the text.

PEU/3 wt% POSS and PEU/6 wt% POSS formed continuous entireties with "cavities" of different sizes (Fig. 9, c and d, indicated by arrow heads). The cells, as judged by the position of their nuclei, are either located on the top of the polymer or in the cavities of the polymer matrices (Fig. 9, b, c, d). When examined under a fluorescence microscope with filters set for fluorescein isothiocyanate (FITC), the polymers gave bright green fluorescence that produced images reflecting the detailed surface topography of polymer matrices (Fig. 9, b′, c′, d′, Fluo). The fluorescent images clearly demonstrate that incorporation of POSS into PEU changed the surface structure of the polymers. The cavities or groves are clearly revealed in PEU/3 wt% POSS and PEU/6 wt% POSS thin films (Fig. 9, c′ and d′, indicated by arrow heads). It is noted that PEU/6 wt% POSS formed a 3-dimensional matrix with nicely patterned pores and groves (Fig. 9, d′). This is an attractive new feature in the context of tissue engineering since it is this porous nature that allows cells to better access the growth factors/nutrients and communication through secreted signaling molecules among cells at different locations [41].

Previous studies have shown that polyurethanes are biocompatible and do not show cytotoxicity to cells in culture. Therefore,

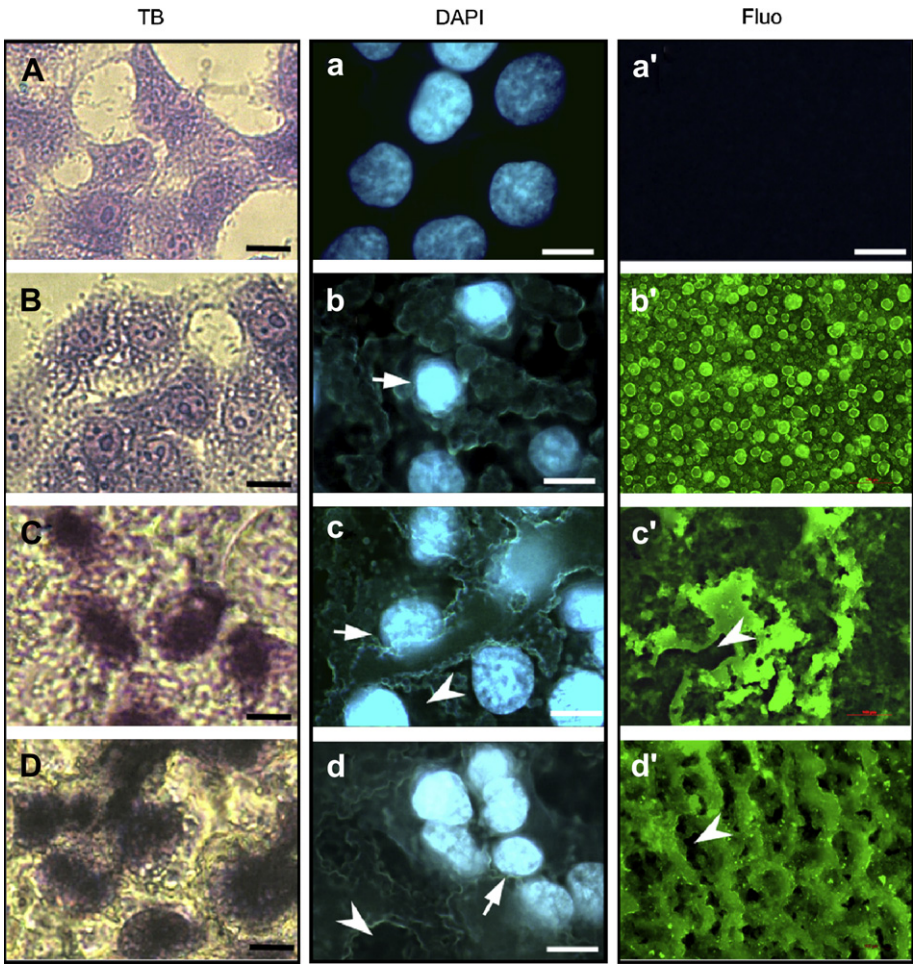

Fig. 9. Microscopic analysis of cell morphology and surface structure of the PEU and PEU/POSS matrices. KB cells grown on cell culture coverglasses (A, a, a′), PEU film (B, b, b′), PU/3%POSS (C, c, c′) and PU/6%POSS (D, d, d′). A–D, toluidine blue stained cells (TB, scale bars = 10 μm). a–d, DAPI stained nuclei (DAPI, scale bars = 10 μm). b′, c′, and d′ represent the intrinsic fluorescence of the polymers detected under a fluorescence microscope with a FITC filter set (scale bars = 100 μm). The coverglass (a′) did not emit detectable fluorescence.

they have been used to develop materials for biomedical devices or other medical applications [42]. However, there are some concerns regarding its resistance to degradation in vivo. Thus there is a need to improve the stability of existing PEU. The data presented in this study demonstrate that the POSS incorporated into PEU does not interfere with cell adhesion or cause cytotoxicity. In addition to its improved chemical and physical properties, an important finding is that PEU/POSS nanocomposites seem to have architectures that favor cell–polymer interaction. It is conceivable that the porous polymer scaffolds may facilitate nutrient/waste exchange and cell morphogenesis and remodeling, allowing tissue regeneration in vivo. Therefore, the high porosity of PEU/POSS nanocomposite represents an excellent property for its potential biomedical applications.

The surface structure features revealed under a fluorescence microscope were unexpected. These images give detailed surface topography that, in fact, resembles the 3-dimensional images of POSS/poly(carbonate-urea) nanocomposites generated from a scanning electron microscope as described by Kannan et al. [39]. While the exact structures responsible for fluorescence emission remains to be determined, its fluorescence nature has been reported [43]. Therefore, fluorescence microscopy can be a useful tool to visualize the three-dimensional surfaces of PEU/POSS nanocomposites, making it possible to understand and interpret the role of critical interfacial phenomena and surface topography in interaction between cells and extracellular matrix (ECM) that supports the cell growth.

4. Conclusions

A new type of a polymer nanocomposite system was prepared by chemically reacting POSS with dihydroxyl functional group with biodegradable and biocompatible poly(ester urethane) (PEU) via *in situ* homogeneous solution polymerization. The structure, properties and cell compatibility of the PEU/POSS nanocomposite were investigated. The results show that the glass transition temperatures and thermal stability of the nanocomposites increase with increasing POSS content. Compared with the pure PEU, PEU/POSS nanocomposites have higher modulus and tensile strength. The degradation resistance of the nanocomposites is enhanced by incorporating POSS into the PEU. Cell culture studies revealed that incorporation of POSS into PEU did not significantly affect cell attachment and cell viability while the surface structure of the PEU/POSS nanocomposite system changed significantly by incorporating POSS, allowing the formation of highly porous matrix that may potentially enhance biocompatibility. This work points to an important and facile strategy for preparing useful synthetic polymers with prescribed macromolecular structure and biological function for possible uses in biomedical and tissue engineering applications where current commercial polyurethanes may not be useable.

Acknowledgments

This work was primarily supported by the Chemical, Bioengineering, Environmental, and Transport Systems Division of the U.S. National Science Foundation under award number CBET 0752150. We thank Hybrid Plastics (Hattiesburg, Mississippi) for donation of the POSS chemicals and technical assistance. We also thank Baobin Kang for microscopy analysis and Mississippi Functional Genomics Network for the use of the facility. J.U.O. acknowledges the research work of his former graduate students and postdocs.

References

[1] Madbouly SA, Otaigbe JU. Macromol Chem Phys 2006;207:1233–43.
[2] Madbouly SA, Otaigbe JU. Polymer 2007;48:4097–107.
[3] Alam TM, Otaigbe JU, Rhoades D, Holland GP, Cherry BR, Kotula PG. Polymer 2005;46:12468–79.
[4] Lichtenhan JD, Haddad TS, Scwab JJ, Carr MJ, Chaffee KP, Mather PT. Polym Preprints Am Chem Soc 1998;215:218.
[5] Lichtenhan JD. Comments Inorg Chem 1995;17:115–30.
[6] Kannan RY, Salacinski HJ, Butler PE, Seifalian AM. Acc Chem Res 2005;38:879–84.
[7] Gao H, Ji B, Jager IL, Arzt E, Fratz P. Proc Natl Acad Sci USA 2003;100:5597–600.
[8] Arroyo-Hernández M, Pérez-Rigueiro J, Manso-Silván M, Martínez Duart JM. Mater Sci Eng C 2007;27:1211–4.
[9] Canham LT, Reeves CL, Newey JP, Houlton MR, Cox TJ, Buriak JM, et al. Adv Mater 1999;11:1505.
[10] Knight PT, Lee KM, Qin H, Mather PT. Biomacromolecules 2008;9:2458–67.
[11] Lee KM, Knight PT, Chung T, Mather PT. Macromolecules 2008;41:4730–8.
[12] Guelcher SA. Tissue Eng Part B Rev 2008;14:3–17.
[13] Chen QZ, Bismarck A, Hansen U, Junaid S, Tran MQ, Harding SE, et al. Biomaterials 2008;29:47–57.
[14] Lelah MD, Cooper JL. Polyurethanes in medicine. Boca Raton, FL: CRC Press; 1987.
[15] Matheson LA, Santerre JP, Labow RS. J Cell Physiol 2004;199:8–19.
[16] Simmons A, Padsalgikar AD, Ferris LM, Poole-Warren LA. Biomaterials 2008;29:2987–95.
[17] Wang W, Guo Y, Otaigbe JU. Polymer 2008;49:4393–8.
[18] Seifalian AM, Salacinski HJ, Tiwari A, Edwards A, Bowald S, Hamilton G. Biomaterials 2003;24:2549–57.
[19] Jones JA, Dadsetan M, Collier TO, Ebert M, Stokes KS, Ward RS, Hiltner PA, Anderson JM. J Biomater Sci Polym Ed 2004;15:567–87.
[20] Nanda AK, Wicks DA, Madbouly SA, Otaigbe JU. Macromolecules 2006;39:7037–43.
[21] Madbouly SA, Otaigbe JU, Nanda AK, Wicks DA. Macromolecules 2007;40:4982–91.
[22] Kannan RY, Salacinski HK, De Groot J, Clatworthy I, Bozec L, Hortin M, et al. Biomacromolecules 2006;7:215–23.
[23] Lichtenhan JD, Vu NQ, Carter JA, Gilman JW, Feher FJ. Macromolecules 1993;36:2141–2.
[24] Lichtenhan JD, Otonari YA. Macromolecules 1995;28:8435–7.
[25] Tsuchida A, Bolln C, Sernetz FG, Frey H, Muelhaupt R. Macromolecules 1997;30:2818–24.
[26] Mather PT, Jeon Hong A, Romo-Uribe A, Haddad TS, Lichtenhan JD. Macromolecules 1999;32:1194–203.
[27] Pielichowski K, Njuguna J, Janowski B, Pielichowski J. Adv Polym Sci 2006;201:225–96.
[28] Lichtenhan JD. In: Salmone JC, editor. Silsesquioxane-based polymers. Polymeric materials encyclopedia, vol. 10. CRC Press; 1996. p. 7768–78.
[29] Neumann D, Fisher M, Tran L, Matisons JG. J Am Chem Soc 2002;124:13998–9.
[30] Turri S, Levi M. Macromol Rapid Commun 2005;26:1233–6.
[31] Fu BX, Hsiao BS, Pagola S, Stephens P, White H, Rafailovich M, et al. Polymer 2001;42:599–611.
[32] Rubinstein M, Colby RH. Polymer physics. Oxford; 2003. See also: Bower DI. An introduction to polymer physics. Cambridge University Press; 2002.
[33] Struik LCE. Physical aging in amorphous polymers and other materials. Elsevier; 1978. See also: Ferry JD. Viscoelastic properties of polymers. 3rd ed. Wiley; 1980.
[34] Xu HY, Yang BH, Wang JF, Guang SY, Li C. Macromolecules 2005;38:10455–60.
[35] Liu YR, Huang YD, Liu L. J Mater Sci 2007;42:5544–50.
[36] Lee YJ, Kuo SW, Huang CF, Chang FC. Polymer 2006;47:4378–86.
[37] Choi J, Kim SG, Laine RM. Macromolecules 2004;37:99–109.
[38] Liu HZ, Zheng SX. Macromol Rapid Commun 2005;26:196–200.
[39] Kannan RY, Salacinski HJ, Odlyha M, Butler PE, Seifalian AM. Biomaterials 2006;27:1971–9.
[40] Lee PC, Chen LW, Lin JR, Hsieh KH, Huang LLH. Polym Int 1996;41:419–25.
[41] Burdick JA, Vunjak-Novakovic G. Tissue Eng Part A 2000;14:1–14.
[42] Lambda NMK, Woodhouse KA, Cooper SL. Polyurethanes in biomedical applications. CRC Press; 1998.
[43] Krucker T, Lang A, Meyer EP. Microsc Res Tech 2006;69:138–47.